



# CHALMERS

## Chalmers Publication Library

### Computational optimization of catalyst distributions at the nano-scale

This document has been downloaded from Chalmers Publication Library (CPL). It is the author's version of a work that was accepted for publication in:

**Applied Energy (ISSN: 0306-2619)**

Citation for the published paper:

Ström, H. (2015) "Computational optimization of catalyst distributions at the nano-scale".  
Applied Energy

<http://dx.doi.org/10.1016/j.apenergy.2015.10.171>

Downloaded from: <http://publications.lib.chalmers.se/publication/225120>

Notice: Changes introduced as a result of publishing processes such as copy-editing and formatting may not be reflected in this document. For a definitive version of this work, please refer to the published source. Please note that access to the published version might require a subscription.

Chalmers Publication Library (CPL) offers the possibility of retrieving research publications produced at Chalmers University of Technology. It covers all types of publications: articles, dissertations, licentiate theses, masters theses, conference papers, reports etc. Since 2006 it is the official tool for Chalmers official publication statistics. To ensure that Chalmers research results are disseminated as widely as possible, an Open Access Policy has been adopted. The CPL service is administrated and maintained by Chalmers Library.

(article starts on next page)

# 1 Computational optimization of catalyst distributions at the 2 nano-scale

3  
4 Henrik Ström<sup>a,b,\*</sup>

5  
6 <sup>a</sup>*Department of Applied Mechanics, Chalmers University of Technology, Gothenburg SE-412  
7 96, Sweden*

8 <sup>b</sup>*Department of Energy & Environment, Chalmers University of Technology, Gothenburg SE-  
9 412 96, Sweden*

10 <sup>\*</sup>*Corresponding author: [henrik.strom@chalmers.se](mailto:henrik.strom@chalmers.se); +46317721360*

## 11 12 13 **Abstract**

14  
15 Catalysis is a key phenomenon in a great number of energy processes, including feedstock  
16 conversion, tar cracking, emission abatement and optimizations of energy use. Within  
17 heterogeneous, catalytic nano-scale systems, the chemical reactions typically proceed at very  
18 high rates at a gas-solid interface. However, the statistical uncertainties characteristic of  
19 molecular processes pose efficiency problems for computational optimizations of such nano-  
20 scale systems. The present work investigates the performance of a Direct Simulation Monte  
21 Carlo (DSMC) code with a stochastic optimization heuristic for evaluations of an optimal  
22 catalyst distribution. The DSMC code treats molecular motion with homogeneous and  
23 heterogeneous chemical reactions in wall-bounded systems and algorithms have been devised  
24 that allow optimization of the distribution of a catalytically active material within a three-  
25 dimensional duct (e.g. a pore). The objective function is the outlet concentration of  
26 computational molecules that have interacted with the catalytically active surface, and the  
27 optimization method used is simulated annealing. The application of a stochastic optimization  
28 heuristic is shown to be more efficient within the present DSMC framework than using a  
29 macroscopic overlay method. Furthermore, it is shown that the performance of the developed  
30 method is superior to that of a gradient search method for the current class of problems.  
31 Finally, the advantages and disadvantages of different types of objective functions are  
32 discussed.

33  
34 **Keywords:** Optimization; DSMC; Catalysis; Stochastic optimization; Nanoscale  
35

---

36 This paper was presented at the 7th International Conference on Applied Energy (ICAE2015),  
37 March 28-31, 2015, Abu Dhabi, UAE (Original paper title: “A computational method to  
38 optimize the distribution of a catalytically active material inside a nano-scale pore” and Paper  
39 No.: 173).

## 40 **1. Introduction**

41

42 The most viable route to a reduction of the environmental costs of modern societies is an  
43 increase in the efficiencies of processes used in the manufacturing and transportation of  
44 products and in the production of energy [1]. Catalysis is a key phenomenon in a great  
45 number of relevant industrial processes, including feedstock conversion [2, 3], energy  
46 conversion [4], tar cracking [5], emission abatement [6, 7] and optimizations of energy use  
47 [8]. At the same time, nanotechnology has emerged as a subject area with a strong potential to  
48 enhance energy efficiency in all areas of the energy sector, from energy sources to energy  
49 change, distribution, storage and usage [9]. It now seems clear that the future development  
50 and optimization of fields such as renewable energy production and emission abatement will  
51 depend on the success of research activities related to reactive systems at the nano-scale.

52

53 More specifically, the current development of heterogeneous catalysis at the nano-scale is  
54 particularly promising [7]. Within heterogeneous, catalytic nano-scale systems, the chemical  
55 reactions are allowed to proceed at very high rates at a gas-solid interface (often the surface of  
56 a precious metal). The process efficiency is limited by the acceptable cost of the particular  
57 material in combination with the surface-to-bulk atom ratio obtainable, since the chemical  
58 reaction only occurs at the surface and the interior atoms remain unused. As the gas  
59 containing the reactants is typically brought into contact with the catalyst while being forced  
60 to flow past it, optimization of the efficiencies of such systems require numerical tools that  
61 take into account both the chemistry and the fluid dynamics of the system.

62

63 The governing processes in applications where the bounding geometry is of micro- or  
64 nanometer size typically span several orders of magnitude in spatial and temporal scales [10-  
65 12]. Consequently, there are many inherent difficulties involved in performing non-intrusive,  
66 non-destructive experimental investigations of the processes occurring on the smallest scales  
67 in such systems. Comprehensive numerical models therefore form an indispensable basis in  
68 the research into their behavior.

69

70 The multi-scale nature of heterogeneous catalytic systems has led to the development of a  
71 number of numerical frameworks dedicated to their study. Multi-scale models for reaction and  
72 transport in porous catalysts that are based on the continuum assumption have been proposed  
73 by several authors [13, 14]. However, such methods rely on the use of effective transport  
74 coefficients in macroscopic balance equations and cannot be used for systems where there is a  
75 net convective flow when the mean free path is significant to the bounding geometry (e.g.

76 when the Knudsen number is larger than 0.015) [15]. For such systems, continuum  
77 descriptions are not valid, and the predicted velocity fields are therefore erroneous, leading to  
78 inaccurate predictions of momentum, heat and mass transfer. The route to accurate  
79 descriptions of molecular flows with chemical reactions is via molecular methods, e.g. by  
80 obtaining the solution to the Boltzmann equation rather than the Navier-Stokes equations [15-  
81 18]. Solving the Boltzmann equation directly is however very difficult for real-world  
82 problems, as it represents a 7D partial differential equation (for the probability distribution of  
83 molecular positions and velocities over time). A more efficient approach is then to use a  
84 molecular simulation model, such as Direct Simulation Monte Carlo (DSMC) [19]. It has  
85 been shown that the DSMC method can be directly related to the Boltzmann equation and that  
86 solutions from the two frameworks are consistent [20, 21]. Furthermore, the DSMC method  
87 has the additional advantages of allowing treatment of inverse collisions and ternary chemical  
88 reactions, which becomes especially problematic in attempts at solving the Boltzmann  
89 equation directly [19]. The DSMC method is therefore well suited to describe reactive nano-  
90 scale systems [12, 22]. It is, in fact, the most widely used numerical algorithm in kinetic  
91 theory [23, 24] and has been experimentally validated for a great number of applications,  
92 including nonequilibrium gas flows (e.g. shocks) [24], rarefied gas dynamics (e.g. velocity,  
93 temperature and concentration slip) [25], near-vacuum flow of high-temperature gas at  
94 supersonic speeds [26], low-pressure deposition processes [27] and temperature-programmed  
95 desorption in heterogeneous catalysis [12].

96  
97 A scientific problem of specific interest for heterogeneous catalytic systems is that of  
98 optimizing the catalyst distribution. In such an optimization process, the goal is to come up  
99 with a conceptual solution for the optimal design of the catalytic system, within a given  
100 design space while respecting a set of design constraints. Fine-tuning of the system with  
101 respect to actual real-life performance and manufacturability can then be carried out from an  
102 otherwise optimal starting point, resulting in significant reductions of the total development  
103 time and cost. However, most state-of-the-art optimization methods developed for reactive  
104 fluid flow systems rely on the availability of a system of partial differential equations  
105 describing the system in question. Hence, when the system to be optimized is described by a  
106 molecular method instead, many well-known optimization methods (such as the adjoint  
107 method for aerodynamic shape optimization [28, 29]) cannot be applied directly. Furthermore,  
108 as one of the most prominent characteristics of molecular systems is the existence of  
109 statistical uncertainties [30, 31], any chosen objective function will always contain some  
110 degree of noise. In the optimization of a reactive nano-scale system, it is therefore reasonable  
111 to choose an optimization heuristic that can find the approximate global optimum while

112 handling uncertainties in the objective function and discrete search spaces. One optimization  
113 heuristic that fulfils these requirements is the stochastic optimization approach known as  
114 simulated annealing [32, 33]. The simulated annealing method is simple to implement,  
115 relatively fast and has been found to be more accurate than genetic algorithms and maximum  
116 entropy reconstruction techniques in reconstructions of heterogeneous media [34].  
117 Interestingly, the simulated annealing method itself is also classified as a Monte Carlo  
118 method, as it constitutes an adaptation of the Metropolis-Hastings algorithm [35].

119  
120 There have been previous attempts at using the DSMC method in optimization studies.  
121 Recently, Pflug et al. [36] used DSMC to optimize the film thickness uniformity in an  
122 industrial physical vapor deposition (PVD) reactor. However, the design of the PVD reactor  
123 in question allowed for a single DSMC computation to be used (per sputtering material) to  
124 optimize the geometry. For a generic heterogeneous catalytic system, such simplifications are  
125 typically not possible. Furthermore, enumeration approaches (repeating simulations for  
126 several values of a given design parameter) can be useful for systems that are easily  
127 characterized by a small set of design parameters [cf. 37], but are also not generally applicable  
128 to problems involving the distribution of a catalytic material over the walls of a fixed system,  
129 as the possible designs are too many and cannot easily be grouped together.

130  
131 Hence, the purpose of the present work is to develop a numerical tool for investigations of  
132 reacting, molecular flows that can be applied in optimizations of catalytic systems on the  
133 micro- and nano-scales. The main challenge to be faced is thus related to the inevitable  
134 fluctuations in any objective function that result from the natural uncertainty pertaining to the  
135 molecular regime: when the continuum approximation no longer holds, fluctuations appear in  
136 the macroscopic properties derived by averaging over molecular properties [38]. It is shown  
137 in the current work that a successful (i.e. robust and computationally efficient) optimization  
138 approach for such cases is dependent on a well-balanced combination of the choice of  
139 objective function, optimization algorithm and convergence criteria.

140

141

## 142 **2. Modeling**

143

### 144 **2.1. The Direct Simulation Monte Carlo (DSMC) framework**

145

146 The route to accurate descriptions of molecular flows with chemical reactions is via molecular  
147 methods, e.g. by obtaining the solution to the Boltzmann equation rather than the Navier-

148 Stokes equations [15-18]. The molecular method chosen in the present work is the well-  
149 established Direct Simulation Monte Carlo (DSMC) method [19], which is a probabilistic  
150 simulation approach. The fluid flow is modelled using particles that represent a large number  
151 of real molecules. The particle motion is updated deterministically using a time step that is  
152 smaller than the mean collision time, so that the intermolecular collisions can be decoupled  
153 from the molecular motion. The code developed in this work is based on Bird's DSMC  
154 method [19] and is able to handle chemistry in the gas phase and to approximate the rate of  
155 surface chemistry reactions at gas-solid interfaces [39, 40]. More specifically, the code is  
156 designed for performing optimizations of the distribution of an active material over the  
157 bounding surfaces of the system. The aim is to make possible a complete optimization during  
158 the course of one single simulation run. The code is written in the programming language C.

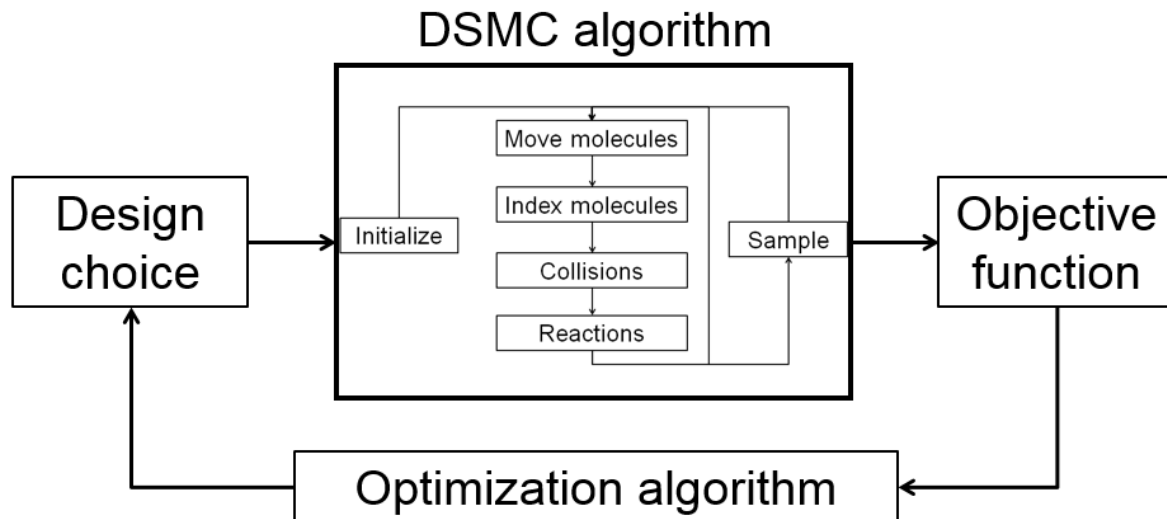
159

160 The DSMC procedure has been described extensively elsewhere [19], and will only be  
161 summarized briefly here. With DSMC, the ensemble of molecules is modeled with a reduced  
162 number of computational molecules that move in straight lines according to their velocities  
163 for a short time step during which no collisions take place. Thereafter, collisions are modelled  
164 using random numbers and collision probabilities, which are based on the collision cross  
165 section and the relative velocities between pairs of molecules. Here, the hard sphere model is  
166 used to determine the outcome of a collision (scattering angles and post-collision velocities)  
167 [19], as it is sufficient for the purpose of the present work. If a molecule collides with a wall,  
168 an adsorption or wall reaction event can be triggered, and if two molecules collide, a  
169 homogeneous chemical reaction can result.

170

171 At certain intervals, sampling is performed over the molecules to derive the macroscopic  
172 fields of interest, such as the mass-averaged gas velocity, temperature and species or number  
173 concentrations. This sampling is performed on a computational mesh that is coarser than the  
174 mesh used to calculate collisions, and the two types of cells are typically referred to as cells  
175 (or samplings cells) and subcells (or collision cells), respectively. The flow is sampled every  
176 fourth time step to obtain samples with only a small degree of correlation. A schematic  
177 diagram of the DSMC algorithm within the layout of the complete code is shown in Figure 1.

178



179

180

181 **Figure 1.** Schematic layout of the DSMC algorithm and the optimization algorithm and their  
 182 interconnectedness.

183

184

## 185 2.2. The stochastic optimization heuristic

186

187 Macroscopic fields in a DSMC procedure are always deduced by averaging over the  
 188 computational molecules and therefore have a tendency to contain statistical scatter, as the  
 189 presence of a statistically significant number of molecules in all sampling cells at all times  
 190 cannot be guaranteed [30]. (On the contrary, it is precisely this loss of statistically significant  
 191 averages that causes the continuum approximation to break down and that therefore  
 192 characterizes the molecular flow regimes). This problem becomes further emphasized with  
 193 the DSMC method, since the actual number of real molecules is represented by a smaller  
 194 number of computational molecules, which acts so as to increase the scatter [31]. In addition,  
 195 the objective function in the optimization process may very well exhibit both global and local  
 196 optima. Furthermore, it is not possible to test every conceivable geometrical design due to the  
 197 large computational cost of such an investigation. A suitable compromise is then to use a  
 198 stochastic optimization method, such as simulated annealing [32, 33, 41, 42]. Simulated  
 199 annealing cannot be guaranteed to find the global optimum of an objective function, but it can  
 200 avoid becoming trapped in a local optimum (when there is a better global optimum  
 201 somewhere else), it prevents premature termination due to scatter in the objective function  
 202 and it helps avoid the tedious task of investigating every possible design case.

203

204 In the current work, the following simulated annealing heuristic is used:

- 205 1) Sample the objective function for one initial (randomly chosen) design case.  
206 2) Pick another design case (using an algorithm that has to be specified separately).  
207 3) If the new case is better, move to it. If it is worse, accept it anyway with a certain  
208 probability,  $P$ . This probability is to be a function of the time elapsed in the optimization  
209 process and it too has to be specified separately.  
210 4) Repeat steps 2-3 a pre-determined number of rounds or until the objective function reaches  
211 a pre-defined threshold value.

212

213 At the heart of the simulated annealing algorithm lies the determination of the probability  $P$ .  
214 The original probability function of Kirkpatrick et al. [32] is here modified slightly, so that

215

$$216 \quad P = \exp \left[ \frac{-(f' - f)/f}{T(t)} \right]$$

217

218 In this notation,  $f$  is the value of the objective function, a prime denotes the value for the  
219 newer design case, and  $T(t)$  is the analogue of temperature in a physical annealing process. In  
220 this work, the function  $T(t)$  is defined as

221

$$222 \quad T(t) = a\tau(1 - b t/t_{max})$$

223

224 where  $t$  is the total time elapsed in the simulation and  $t_{max}$  is the time at which the  
225 optimization process is stopped. Hence, the tendency to accept a design case that is worse  
226 decreases with time. The variable  $\tau$  represents the convergence criterion for the normalized  
227 change in the objective function, and the parameters  $a$  and  $b$  thus determine the behavior of  $P$   
228 in time. These values should be chosen to enable a more global character of the search  
229 initially, and to progress towards a local search in the most promising region with time. The  
230 optimum values for a generic problem will always be problem-dependent to some extent. In  
231 the current work, the values  $a = 2$  and  $b = 0.95$  were found to produce satisfactory results.

232

233 The final component in the optimization routine is the algorithm for picking another design.  
234 This component is not prescribed by the simulated annealing algorithm as such, but typically  
235 involves a randomized selection of either the step length, the step direction, or both [41]. The  
236 following algorithm was applied in the present work:

- 237 1) The new design is obtained by moving the catalytically active region of interest a  
238 (uniformly distributed) random distance in the interval  $[\Delta x/20, \Delta x/10]$ , where  $\Delta x$  is the extent  
239 of the domain in coordinate direction  $x$ .



240 2) The direction in which to move is by default the direction of increasing value of the  
241 objective function, but in 25% of the cases the direction is reversed to introduce a random  
242 behavior also to the design picking algorithm.

243 3) Modifications to the new design choice are made if needed to ensure that the geometric  
244 bounds of the system are respected.

245

246 A schematic illustration of the implementation of the optimization algorithm into the DSMC  
247 framework is shown in Figure 1. For every design that is to be evaluated, the DSMC code  
248 needs to run long enough for the samples used to calculate the objective function to converge.  
249 It is therefore evident that the choice of objective function and the robustness of the  
250 optimization algorithm with regard to fluctuations and sampling errors are of utmost  
251 importance in the derivation of the combined procedure.

252

253

### 254 **3. Results and Discussion**

255

256 The DSMC code is validated in an extensive series of tests, of which only a subset are  
257 reported here. Thereafter, the task of finding the optimum position for a catalytically active  
258 region inside a three-dimensional pore is used to test the robustness and efficiency of the  
259 proposed optimization algorithm.

260

261

#### 262 **3.1. Validation of the DSMC code**

263

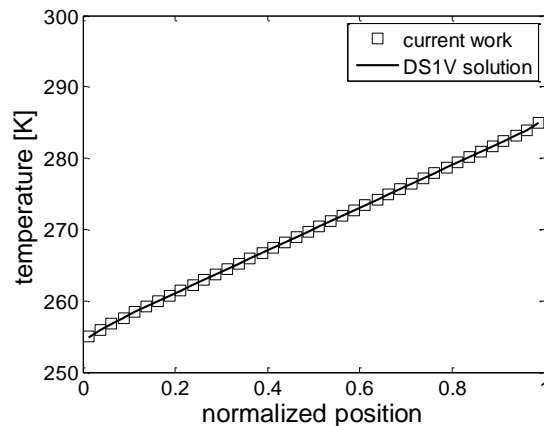
264 As the most challenging aspect of the DSMC procedure in relation to molecular motion lies in  
265 the modelling of molecular collisions, one fundamental validation test carried out is that of a  
266 homogeneous gas at rest in a one-dimensional domain. This test case proves that the code is  
267 able to predict the correct solution for a one-dimensional homogeneous gas and that the  
268 performance of the random number generator used is acceptable. Indeed, the number of  
269 collisions predicted is very close to the theoretical value [19], and the mean collision  
270 separation is less than 5% of the cell-width, meaning that collision partners are located within  
271 the same subcell.

272

273 Next, the performance of the DSMC code is exemplified for a non-isothermal fluid flow test  
274 case where the domain is a flow between two planes separated by a distance of 0.5 m. This  
275 distance is divided into 40 sampling cells with 10 collision subcells each. The number of

276 computational molecules is  $10^5$ , and the number density of molecules is  $10^{20} \text{ m}^{-3}$ . The  
277 Knudsen number is approximately 0.03. The lower wall is stationary and maintained at a  
278 temperature of 250 K. It has surface properties such that 50% of the incoming molecules are  
279 specularly reflected, whereas the rest are diffusively reflected. The upper wall is maintained at  
280 300 K and moves at a velocity of 1 m/s in the plane perpendicular to the gap. At this wall,  
281 80% of the incoming molecules are specularly reflected. For this problem, the performance of  
282 the current code is validated by comparing its predictions to benchmark results from one of  
283 Graeme Bird's program in the DS suite (DS1V) [43], in line with Bird's recommendation on  
284 how to assess the validity of a new DSMC code. The predicted temperature slip is  
285 approximately 3.4 times higher at the hotter boundary, which agrees well with the DS1V  
286 solution as shown in Figure 2.

287  
288



289  
290

291 **Figure 2.** Sampling cell temperature as a function of the normalized position between a  
292 stationary and a moving wall of different temperatures. The plane at position 0 is maintained  
293 at 250 K and is specularly reflecting to 50% while the plane at position 1 is maintained at 300  
294 K and is specularly reflecting to 80%. The predictions obtained in the current work are in  
295 excellent agreement with the DS1V solution.

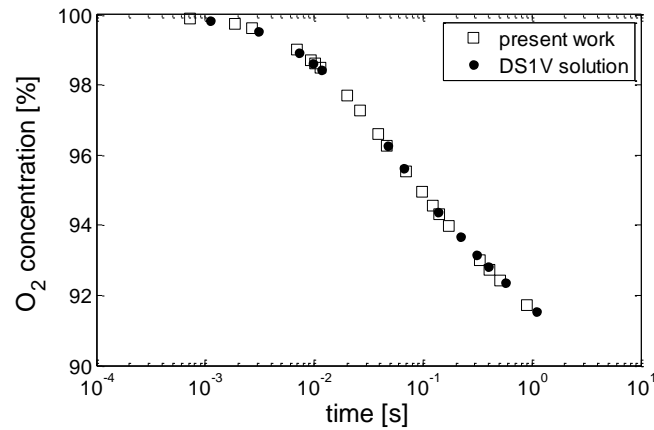
296  
297

298 The ability of the code to handle different molecular species and chemical reactions is  
299 validated in a homogeneous chemistry test case. Two stationary walls are separated by a  
300 distance of 0.5 m. Both walls have surface properties such that there is 100% specular  
301 reflection. The gap between the walls is initially occupied by oxygen ( $\text{O}_2$ ) at a number density  
302 of  $10^{20} \text{ m}^{-3}$  and a temperature of 5000 K. In this test case, two chemical reactions may occur,  
303 namely the dissociation and recombination, respectively, of diatomic oxygen and atomic

304 oxygen:  $O_2 \leftrightarrow 2O$ . The total duration of the simulation is approximately one second of real  
305 time, and the result is shown in Figure 3. Again, the current code is in excellent agreement  
306 with the DS1V solution.

307

308



309

310 **Figure 3.** Volume-averaged concentration of diatomic oxygen as a function of time. The gas  
311 consists of 100% pure  $O_2$  initially. The predictions obtained in the current work are in  
312 excellent agreement with the corresponding DS1V solution.

313

314

315 A comprehensive treatment of surface reactions in the DSMC framework would necessitate  
316 detailed modeling of adsorption, desorption, coadsorption, reaction, surface diffusion and the  
317 effects of surface defects, which is currently beyond the state-of-the-art for this computational  
318 technique, although significant advances are made continuously [12]. Such additional  
319 complexities would also add to the computational cost and significantly reduce the efficiency  
320 of the optimization. In this work, surface reactions are therefore instead implemented as  
321 occurring at a wall with a certain probability [40]. This probability can be tuned to reproduce  
322 a physical reaction rate, implying that the main simplification involved is related to the loss of  
323 coverage-dependence. This simplification is deemed appropriate in the light of the main goal,  
324 which is to combine the DSMC simulation with an inline optimization routine.

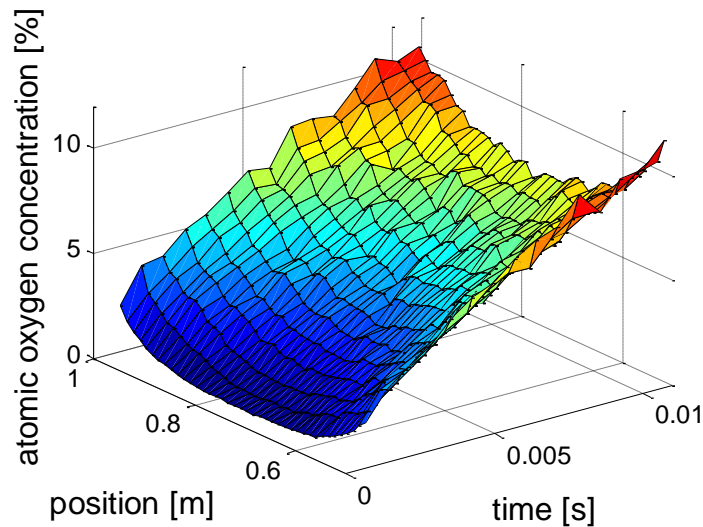
325

326 As a test case for the surface reaction setup, the wall-catalyzed dissociation of oxygen is  
327 simulated at a temperature of 300 K in the same geometry as the homogeneous validation  
328 case. Dissociation is prescribed to occur at the walls with a reaction probability of 1%. The  
329 temporal evolution of the atomic oxygen concentration profile is depicted in Figure 4. The  
330 results presented here agree with what is qualitatively expected for the system under

331 investigation and thus constitute a verification of the implementation of the wall reaction  
332 mechanism into the code.

333

334



335

336

337 **Figure 4.** 3D surface plot showing the time-and-space resolved atomic oxygen concentration  
338 in the heterogeneous chemistry test case. The gas is initially pure diatomic oxygen ( $O_2$ ). Upon  
339 collision with a wall, there is a 1% probability that a diatomic oxygen molecule dissociates  
340 ( $O_2 \leftrightarrow 2O$ ). The code predicts that the concentration of atomic oxygen resulting from this  
341 dissociation increases with time and penetrates into the domain.

342

343

344 In conclusion, the observations from these validation tests support the inference that the code  
345 can be used for the optimization processes described next.

346

347

### 348 **3.2. Optimization of the position of a catalytically active region**

349

350 A three-dimensional nano-scale “pore” can be constructed by having two boundaries specified  
351 as an inlet and an outlet, and a procedure is implemented by which the pressure difference  
352 between these boundaries is maintained throughout the simulation [44]. The remaining four  
353 sides of the domain are regular walls, which may be designed with or without protrusions.  
354 The aim is to design a numerical framework that can be used to determine the optimal  
355 distribution of a limited amount of catalytically active material over this pore wall surface. To  
356 simplify the problem setup, the catalytically active material is limited to a single surface

357 location, but generalization to an arbitrary number of active sites is straightforward.  
358 Consequently, in the simulations presented here, the catalytically active region is a 2 nm thin  
359 section around the perimeter of a rectangular (100 x 100 x 300 nm) 3D pore.

360

361

### 362 *3.2.1 Objective function*

363

364 The most important feature of the objective function is that it converges quickly, which means  
365 that the signal should be strong in comparison to the fluctuations present. A comprehensive  
366 treatment of a catalytic reaction at the active region would have to account for sticking factors  
367 lower than unity [45], temperature-dependence of the chemical reaction rates and changes to  
368 the gas phase composition that could potentially affect the molecular flow field. Such effects  
369 would however tend to increase both the magnitude of the fluctuations (by making the  
370 objective function signal lower because of the lower reaction probability) and to delay the  
371 convergence towards a steady state (by introducing changes into the molecular flow field).

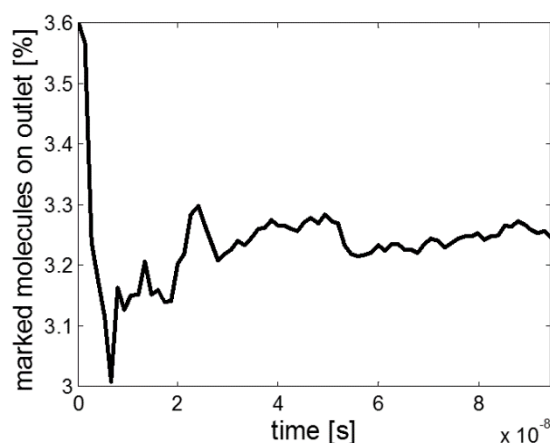
372 For the purpose of optimization, the additional value in terms of the accuracy possibly gained  
373 from adding such descriptions is small in relation to the computational cost. Hence, in the  
374 current work, the chemical reaction is assumed not to influence the molecular flow field. In  
375 other words, no actual reaction (wherein molecules change nature) is carried out, but the  
376 molecules that have made contact with the catalytically active surface are marked, so that  
377 their concentration can be monitored by the code. This approach is equivalent to monitoring  
378 the impingement rate on the catalytically active sites, rather than the actual reaction rate [46].  
379 Under the assumption that the flow field does not change significantly with the trace species  
380 conversion, this method may thus reduce the computational cost of obtaining converged  
381 statistics by several orders of magnitude. Additionally, it could be thought of as a means of  
382 probing the mass transfer rate towards the catalytically active sites (e.g., as in CO oxidation  
383 experiments over Pt/Al<sub>2</sub>O<sub>3</sub> catalysts). It is well known that the reduction of the real number of  
384 molecules to a smaller number of computational molecules in DSMC makes the method  
385 sensitive to the prediction of rare events, which have low probability and therefore would  
386 require a large number of computational molecules to be reproduced correctly. A further  
387 advantage with the proposed approach is therefore that it makes use of all computational  
388 molecules, rather than the small fraction that reacts with the catalyst surface upon  
389 impingement.

390

391 The design picking algorithm is implemented to move the catalytically active section around  
392 in the domain. This algorithm waits for a steady signal from the outlet sampling of marked

393 molecules before changing the location of the catalytically active section as proposed by the  
394 simulated annealing algorithm. The objective function is judged to have converged when the  
395 relative change between two samples is less than  $10^{-3}$ . The convergence history for a typical  
396 design with the specified convergence criterion is shown in Figure 5. The simulation for this  
397 design is continued from the last state of the simulation for the previous design. It is clear that  
398 for the objective function to be useful in finding the optimum location, it need not provide a  
399 highly accurate value for the converged number of marked molecules on the outlet. Instead,  
400 the accuracy necessary is determined only by the need to be able to tell two different designs  
401 apart.

402  
403



404

405 **Figure 5.** Visualization of the objective function versus time for a given position of the  
406 catalytically active slit in the 3D pore.

407

408

409 The effect of the number of computational molecules employed on the fluctuations in the  
410 objective function was also investigated, for  $10^3$ ,  $10^4$  and  $2 \cdot 10^4$  molecules, respectively. There  
411 were no significant adverse effect from employing a smaller number of computational  
412 molecules, leading to the decision to use  $10^3$  molecules in the subsequent optimization runs.  
413 For a more complicated pore structure than the current one, the requirements for the number  
414 of computational molecules could possibly increase [47].

415

416 The computational cost for one DSMC run (i.e. one call to the objective function) depends on  
417 the number of computational molecules used, the number of cells used for the discretization  
418 of the computational domain and the time step employed. For a small number of  
419 computational molecules and a small computational domain (as used here), the time step is  
420 the most limiting factor. At atmospheric conditions, the mean collision time is approximately

421  $10^{-10}$  s, implying that the objective function would converge within  $10^4$  time steps (the time  
422 step is of the order of  $10^{-11}$  s and the total time needed somewhat less than  $10^{-7}$  s (cf. Figure  
423 5)). For the chosen design case, the corresponding run-time for one call on a single CPU is  
424 then several hours. However, atmospheric conditions represent an extreme case in the limit of  
425 zero Knudsen number, and lower pressures or higher temperatures reduce this time  
426 significantly. Similarly, much more complex geometries could significantly increase the  
427 number of computational molecules needed, which would increase the computational cost and  
428 probably make parallelization of the DSMC algorithms necessary [48].

429

### 430 *3.2.2 Sample fluctuations*

431

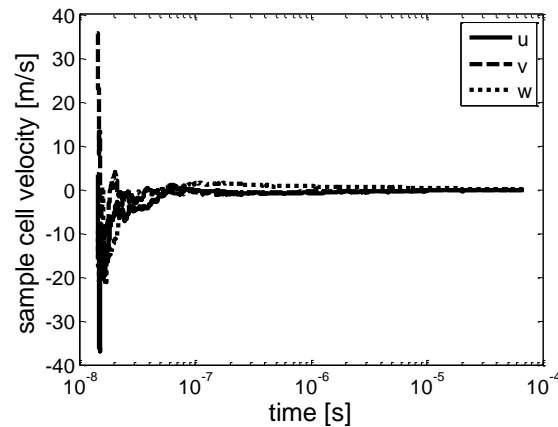
432 Fluctuations in the sampled DSMC properties are the main challenge for the optimization  
433 algorithm. There are macroscopic overlay methods [49, 50] available for the DSCM  
434 framework that are based on the solution of trace species transport equations using the flow  
435 field of the other (dominating) species. Such methods thus represent a solution to the problem  
436 of treating very rare events in DSMC without having to resort to using an excessive number  
437 of computational molecules. However, these approaches are susceptible to numerical errors if  
438 the sampling of the macroscopic fields has not yet converged. This is a significant drawback  
439 in optimization, and it makes these methods less efficient than the sampling of marked  
440 molecules as proposed here.

441

442 As an example, consider the sampling of the three velocity components  $u$ ,  $v$  and  $w$  in a  
443 randomly chosen cell in a three-dimensional pore with a gas at rest at 300 K, as depicted in  
444 Figure 6. It is seen that a total time of 0.1 ms is needed to obtain an estimate of the steady-  
445 state solution which is correct within approximately  $10^{-3}$  m/s. When the simulation is  
446 terminated, hundreds of billions of molecular moves and billions of collisions have been  
447 performed, but mass conservation is still only within 0.1% error tolerance. Errors of such  
448 magnitude are still too large to be acceptable in the solution of a species transport equation  
449 with chemical reaction source terms for a species present in trace amounts.

450

451



452

453

454 **Figure 6.** Convergence history for the three sample velocity components in a randomly  
 455 chosen cell in a  $1 \times 1 \times 3 \mu\text{m}$  domain (discretized into  $8 \times 8 \times 24$  sampling cells). All velocity  
 456 components tend to zero as time increases, which is the result expected for a gas at rest.

457

458

### 459 3.2.3 Optimization

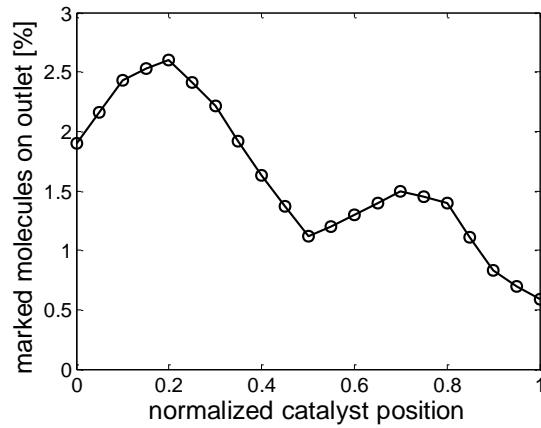
460

461 The optimization algorithm is evaluated for an objective function that contains two local  
 462 optima (and three extreme points), as depicted in Figure 7. The global optimum is positioned  
 463 around  $z = 0.2$  and is  $\sim 2.6\%$ , where  $z$  is the normalized position of the catalytically active slit  
 464 in the streamwise direction. There is also a local maximum ( $\sim 1.5\%$ ) at around  $z = 0.7$ . Figure  
 465 7 represents the converged objective function, but for any sampling from a DSMC simulation  
 466 there will always be a significant uncertainty due to the presence of noise in the signal. This  
 467 noise emanates from the molecular uncertainties and is further influenced by the convergence  
 468 criteria used: in order for computational efficiency not to be lost, the sampling that produces  
 469 the objective function signal has to be terminated within a realistic time frame, and so the  
 470 signal will always be somewhat colored by noise. The extreme point that separates the curves  
 471 leading to the two maxima is located at  $z = 0.5$ . Hence, for the current objective function –  
 472 and in the absence of noise – a gradient search optimization process starting from a random  
 473 location would find the global optimum in 50% of the cases and the other maximum in the  
 474 remaining 50% of the cases. The aim here is to prove that the simulated annealing algorithm  
 475 can exhibit superior performance to such an algorithm.

476

477





478

479 **Figure 7.** Objective function with two local optima, but only one global, and three extreme  
 480 points.

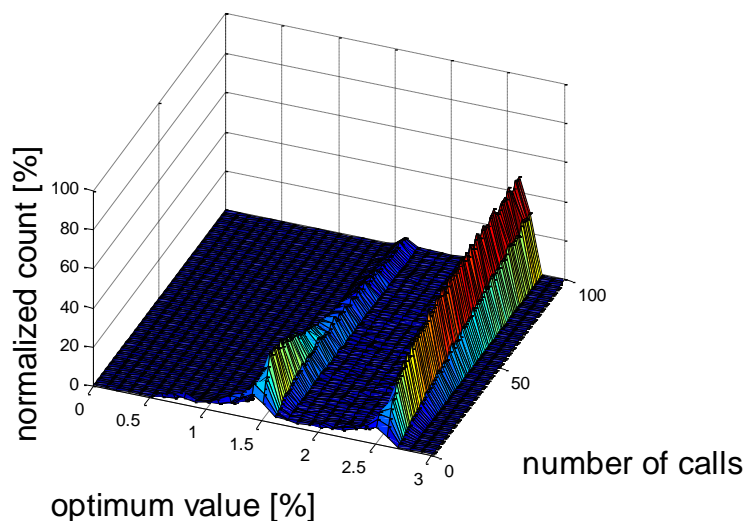
481

482

483 The statistics for the results of the simulated annealing algorithm when applied to a system  
 484 that is described by the aforementioned objective function are shown in Figure 8. The  
 485 optimization process has been repeated 1000 times for every limit on the number of calls to  
 486 obtain reliable statistics. The algorithm is typically able to find the correct optimum after 20  
 487 function calls. As the total number of calls allowed increases, the number of unsuccessful  
 488 simulation runs decreases significantly. This behavior is superior to the performance of a  
 489 gradient search method. A gradient search would only be able to find the local optimum  
 490 closest to the initial position (and only if allowed a large enough number of calls), and would  
 491 not in general be able to handle the fluctuations in the objective function. Consequently, a  
 492 gradient search method could at best produce two ridges of equal height in Figure 8.

493

494



495

496 **Figure 8.** Statistics for the simulated annealing algorithm developed in the present work for  
 497 the objective function in Figure 7.

498

499

500 Finally, it should be stressed here that the number of calls needed to find the correct optimum  
 501 is much dependent on the convergence criterion for the objective function (cf. Section 3.2.1).  
 502 If this convergence criterion is relaxed, each function call will be cheaper but more function  
 503 calls will be needed. Similarly, if the convergence criteria is tightened, the number of calls  
 504 needed will decrease further, at the expense of a higher computational cost for each call. The  
 505 optimum settings for the optimization algorithm itself will therefore depend mostly on the  
 506 signal-to-noise ratio of the objective function chosen for the system under study. Furthermore,  
 507 the computational cost for the DSMC simulation is approximately proportional to the number  
 508 of computational molecules employed, implying that one would like to use as few molecules  
 509 as possible. At the same time, however, the time needed to obtain statistically converged  
 510 DSMC results increases with decreasing the number of computational molecules. In practice,  
 511 the applicability of the DSMC approach is therefore mainly limited by the restriction that the  
 512 time step must be smaller than the collision time, which implies that weakly rarefied flows  
 513 (where the number density of molecules is relatively high) are much more computationally  
 514 expensive than strongly rarefied flows (where the number density is low). In relation to the  
 515 hierarchy of pores existing in a realistic porous medium, the DSMC technique is therefore  
 516 most suited to study the behavior in the smaller pores, although it should be stressed that there  
 517 are no limitations to the validity of the approach for the entire range of pore sizes. For the  
 518 methodology developed in the current work to be more efficiently applied to a large  
 519 computational domain spanning a wide pore size distribution, it is likely that some kind of  
 520 hybrid DSMC/CFD (computational fluid dynamics) method would be most appropriate [51].

521

## 522 **4. Conclusions**

523

524 A Direct Simulation Monte Carlo (DSMC) code has been developed that treats molecular  
525 motion in wall-bounded systems with homogeneous and heterogeneous chemical reactions. A  
526 simulated annealing optimization algorithm is implemented to allow for optimization of the  
527 distribution of a catalytically active material within a 3D pore where the flow field is  
528 described by the present code. It is shown that the performance of the simulated annealing  
529 method for the current class of problems is superior to that of a gradient search method, in  
530 that it enables optimizations also of systems that exhibit global and local optima as well as  
531 fluctuations. Furthermore, using a stochastic optimization heuristic to handle the presence of  
532 noise in the sampling of the objective function is shown to be more efficient than using a  
533 macroscopic overlay method.

534

535 To minimize the difficulties involved with handling noisy objective functions, the objective  
536 function should be a strong signal, suggesting that probing the mass transfer rate towards the  
537 catalytically active sites is more efficient than trying to approximate the actual surface  
538 reaction rate, as long as the local coverage does not vary significantly with the position of the  
539 catalyst material. The approach described in the present work thus represents a suitable  
540 starting-point for addressing a number of important research challenges involving the  
541 optimization of reacting nano-scale flows and reacting heterogeneous flows with and without  
542 surface diffusion.

543

544

## 545 **Acknowledgements**

546

547 This work was financed by a pilot project grant from the Chalmers e-Science Centre (CheSC).

548

549

## 550 **References**

551

552 [1] Dudukovic MP. Reaction engineering: Status and future challenges. Chem Eng Sci  
553 2010;65:3-11.

554 [2] Lin L, Cunshan Z, Vittayapadung S, Xiangqian S, Mingdong D. Opportunities and  
555 challenges for biodiesel fuel. Appl Energy 2011;88:1020-1031.

- 556 [3] Salmi T. Chemical reaction engineering of biomass conversion. *Adv Chem Eng*  
557 2013;42:195-260.
- 558 [4] Menon, V, Banerjee, A, Dailly, J, Deutschmann, O. Numerical analysis of mass and heat  
559 transport in proton-conducting SOFCs with direct internal reforming, *Appl Energy*  
560 2015;149:161-175.
- 561 [5] Palma CF. Modelling of tar formation and evolution for biomass gasification: A review.  
562 *Appl Energy* 2013;111:129-141.
- 563 [6] Liang Z, Ma X, Lin H, Tang Y. The energy consumption and environmental impacts of  
564 SCR technology in China. *Appl Energy* 2011;88:1120-1129.
- 565 [7] Chalmers University of Technology, Studies of individual nanoparticles can be the key to  
566 future catalysis, [https://www.chalmers.se/en/departments/ap/news/Pages/Langhammer-  
567 KAW.aspx](https://www.chalmers.se/en/departments/ap/news/Pages/Langhammer-KAW.aspx), 2015 (Accessed on 2015-10-27).
- 568 [8] Rahimpour MR, Dehnavi MR, Allahgholipour F, Iranshahi D, Jokar SM. Assessment and  
569 comparison of different catalytic coupling exothermic and endothermic reactions: A review.  
570 *Appl Energy* 2012;99:496-512.
- 571 [9] Hessen-Nanotech. Application of nanotechnologies in the energy sector, *Aktionslinie*  
572 *Hessen-Nanotech* 2008;9:1-84.
- 573 [10] Nagel DJ, Zaghoul ME. MEMS: micro technology, mega impact. *IEEE Circuits Syst*  
574 *Mag* 2001;17:14-25.
- 575 [11] Konstandopoulos AG, Kostoglou M. Microstructural aspects of soot oxidation in diesel  
576 particulate filters. *SAE Techn Paper* 2004;01-0693.
- 577 [12] Pesch GR, Riefler N, Fritsching U, Ciacchi LC, Mädler L. Gas-solid catalytic reactions  
578 with an extended DSMC model. *AIChE J* 2015;61:2092-2103.
- 579 [13] Kočí, P, Novák, V, Štěpánek, F, Marek, M, Kubiček, M. Multi-scale modelling of  
580 reaction and transport in porous catalysts. *Chem Eng Sci* 2010;65:412-419.
- 581 [14] Maffei, T, Gentile, G, Rebughini, S, Bracconi, M, Manelli, F, Lipp, S, Cuoci, A, Maestri,  
582 M. A multiregion operator-splitting CFD approach for coupling microkinetic modeling with  
583 internal porous transport in heterogeneous catalytic reactors. *Chem Eng J* 2016;283:1392-  
584 1404.
- 585 [15] Cercignani C. *Rarefied gas dynamics: From basic concepts to actual calculations.*  
586 Cambridge University Press; 2000.
- 587 [16] Bailey CL, Barber RW, Emerson DR. Is it safe to use Navier-Stokes for gas microflows?  
588 European Congress on Computational Methods in Applied Sciences and Engineering,  
589 ECCOMAS; 2004.
- 590 [17] Gu XJ, Emerson DR. A high-order moment approach for capturing non-equilibrium  
591 phenomena in the transition regime. *J Fluid Mech* 2009;636:177-216.

- 592 [18] Xu B, Ju Y. Concentration slip and its impact on heterogeneous combustion in a micro  
593 scale chemical reactor. *Chem Eng Sci* 2005;60:3561-3572.
- 594 [19] Bird G. *Molecular gas dynamics and the direct simulation of gas flows*. Clarendon; 1994.
- 595 [20] Bird, GA. Direct Simulation and the Boltzmann equation. *Phys Fluids* 1970;13:2676-  
596 2681.
- 597 [21] Wagner, W. A convergence proof for Bird's Direct Simulation Monte Carlo method for  
598 the Boltzmann equation, *J Stat Phys* 1992;66:1011-1044.
- 599 [22] Galinsky, M, Sénéchal, U, Breikopf, C. The impact of microstructure geometry on the  
600 mass transport in artificial pores: a numerical approach. *Model Sim Eng* 2014; Article ID  
601 109036, 7 pages.
- 602 [23] Wagner, W. Monte Carlo methods and numerical solutions, *Proc 24<sup>th</sup> Int Symp Rarefied*  
603 *Gas Dynamics, Monopoli (Bari), Italy, 10-16 July, 2004*.
- 604 [24] Erwin, DA, Pham-Van-Diep, GC, Muntz, EP. Nonequilibrium gas flows. I: A detailed  
605 validation of Monte Carlo direct simulation for monatomic gases. *Phys Fluids A* 1991;3:697-  
606 705.
- 607 [25] Wadsworth, DC. Slip effects in a confined rarefied gas. I: Temperature slip. *Phys Fluids*  
608 *A* 1993;5:1831-1839.
- 609 [26] Spencer, RL, Taylor, N, Farnsworth, PB. Comparison of calculated and experimental  
610 flow velocities upstream from the sampling cone of an inductively coupled plasma mass  
611 spectrometer, *Spectrochimica Acta B Atom Spectroscopy* 2009;64:921-924.
- 612 [27] Dorsman, R, Kleijn, CR, Velthuis, JFM, Zijp, JP, van Mol, AMB. Zinc deposition  
613 experiments for validation of direct-simulation Monte Carlo calculations of rarefied internal  
614 gas flows, *J Vac Sci Technol* 2007;25:474-479.
- 615 [28] Jameson, A. *Aerodynamic shape optimization using the adjoint method*, VKI Lecture  
616 *Series on Aerodynamic Drag Prediction and Reduction*, von Karman Institute of Fluid  
617 *Dynamics, Rhode St Genese, 2003*.
- 618 [29] Giannakoglou, KC, Papadimitriou, DI. Adjoint methods for shape optimization, in:  
619 *Optimization and Computational Fluid Dynamics* (eds. Thévenin, D, Janiga, G), Springer  
620 *Verlag, 2008*.
- 621 [30] Plotnikov, MY, Shkarupa, EV. Theoretical and numerical analysis of approaches to  
622 evaluation of statistical error of the DSMC method. *Comp Fluids* 2014;105:251-261.
- 623 [31] Oran, ES, Oh, CK, Cybyk, BZ. *Direct Simulation Monte Carlo: Recent advances and*  
624 *applications*, *Ann Rev Fluid Mech* 1998;30:403-441.
- 625 [32] Kirkpatrick S, Gelatt Jr DA, Vecchi MA. Optimization by simulated annealing. *Science*  
626 1983;220:671-680.

- 627 [33] Černý V. Thermodynamical Approach to the Traveling Salesman Problem: An Efficient  
628 Solution Algorithm. *J Optimiz Theory App* 1985;45:41-51.
- 629 [34] Patelli, E, Schuëller, G. On optimization techniques to reconstruct microstructures of  
630 random heterogeneous media, *Comp Materials Sci* 2009;45:536-549.
- 631 [35] Metropolis, N, Rosenbluth, AW, Rosenbluth, MN, Teller, AH, Teller, E. Equation of  
632 state calculations by fast computing machines. *J Chem Phys* 1953;21:1087-1092.
- 633 [36] Pflug, A, Siemers, M, Melzig, T, Rademacher, D, Zickenrott, T, Vergöhl, M. Numerical  
634 optimization of baffles for sputtering optical precision filters. *Surf Coat Techn* 2014;241:45-  
635 49.
- 636 [37] Wei, J-L, Hu, C-D, Xie, Y-L, Liang, L-Z. Optimization of the gas flow in the  
637 neutralization region of EAST neutral beam injector, *Fusion Eng Des* 2013;88:3176-3179.
- 638 [38] Bird RB, Stewart WE, Lightfoot EN. *Transport phenomena*, 2<sup>nd</sup> Edition. John Wiley &  
639 Sons, Inc.; 2002.
- 640 [39] Herdrich G, Fertig M, Petkow D, Steinbeck A, Fasoulas S. Experimental and numerical  
641 techniques to assess catalysis. *Prog Aerospace Sci* 2012;27:48-49.
- 642 [40] Tomarikawa K, Yonemura S, Tokumasu T, Koido T. Numerical analysis of gas flow in  
643 porous media with surface reaction. *AIP Conf Proc* 2011;1333:796-801.
- 644 [41] Ekren O, Ekren BY. Size optimization of a PV/wind hybrid energy conversion system  
645 with battery storage using simulated annealing. *Appl Energy* 2010;87:592-598.
- 646 [42] Robertson JJ, Polly BJ, Collis JM. Reduced-order modeling and simulated annealing  
647 optimization for efficient residential building utility bill calibration. *Appl Energy*  
648 2015;148:169-177.
- 649 [43] Bird GA. The DS2V/3V Program Suite for DSMC Calculations. *AIP Conf Proc*  
650 2005;762:541-546.
- 651 [44] Wang M, Li Z. Simulations for gas flows in microgeometries using the direct simulation  
652 Monte Carlo method. *Int J Heat Fluid Flow* 2004;25:975-985.
- 653 [45] Steininger H, Lehwald S, Ibach H. On the adsorption of of CO on Pt(111). *Surface Sci*  
654 1982;123:264-282.
- 655 [46] Carlsson P-A, Österlund L, Thormälen P, Palmqvist A, Fridell E, Jansson J, Skoglundh  
656 M. A transient in situ FTIR and XANES study of CO oxidation over Pt/Al<sub>2</sub>O<sub>3</sub> catalysts. *J*  
657 *Catal* 2004;226:422-434.
- 658 [47] Bird, GA. Sophisticated DSMC, DSMC07 Meeting, Santa Fe, 30 September, 2007.
- 659 [48] Roohi, E, Darbandi, M. Recommendations on performance of parallel DSMC algorithm  
660 in solving subsonic nanoflows, *Appl Math Model* 2012;36:2314-2321.
- 661 [49] Boyd ID, Candler GV, Levin DA. Dissociation modeling in low density hypersonic  
662 flows of air. *Phys Fluids* 1995;7:1757-1763.

- 663 [50] Lilley CR, Macrossan MN. A macroscopic chemistry method for the direct simulation of  
664 gas flows. *Phys Fluids* 2004;16:2054-2066.
- 665 [51] Lofthouse, AJ, Boyd, ID, Wright, MJ. Effects of continuum breakdown on hypersonic  
666 aerothermodynamics, AIAA Paper 2006-993.